

Fu Mo Chen

Edge dislocation interacting with a nonuniformly coated circular inclusion

Received: 23 June 2010 / Accepted: 20 August 2010 / Published online: 3 September 2010
© Springer-Verlag 2010

Abstract This paper investigated the interaction between an edge dislocation and a nonuniformly coated circular inclusion. Based on the technique of conformal mapping and the method of analytical continuation in conjunction with alternating technique, the solutions to plane elasticity problems for three dissimilar media are derived explicitly in a series form. For a limiting case when the thickness of the interphase layer is uniform, the derived analytical solutions of this paper are reduced to exactly the same results available in the literature. The image force acting on the dislocation is then determined by using the Peach–Koehler formula. It is found that the combination of material constants and nonuniformity of the interphase thickness will exert a significant influence on the dislocation force.

Keywords Nonuniformly coated circular inclusion · Conforming mapping · Edge dislocation · Analytical continuation · Alternating technique · Image force

1 Introduction

Interactions between dislocations and inhomogeneities have been a topic of considerable research. Solutions of appropriate elasticity problems increase the understanding of material defects and provide an insight into the strengthening and hardening mechanism of materials. A comprehensive survey of the theoretical investigation on this topic has been provided by Dundurs [1]. The force on the dislocation which is near an interface between two dissimilar materials was first treated by Head [2], who considered two infinitely extended solids with a straight interface. He found that the dislocation is either repelled or attracted by the interface, depending on the combination of material constants. Later, these results were used by Fleischer [3] to discuss precipitation hardening of crystals. For the interaction problem of an edge dislocation near a circular inclusion in fiber-reinforced composites, Dundurs and Mura [4] and Dundurs and Sendeckyj [5] indicated that under certain conditions the dislocation may even have a stable equilibrium position at a distance from the circular inclusion interface. The analytical solutions for an inclusion having the elliptic shape were obtained by Warren [6] and by Stagni and Lizzio [7], respectively, for a dislocation acting inside and outside the inclusion. Based on the complex variable approach by Muskhelishvili, Santare and Keer [8] obtained a closed form solution for a dislocation near a rigid elliptical inclusion, in which particular attention is paid to the rigid body rotation of the inclusion relative to the dislocation.

So far, most work on dislocations was restricted to the two-phase (fiber/matrix) model. It is noticed that most of the materials for engineering applications are multiphase systems. And for two-phase materials, when the inclusion phase has finite concentration, dislocation interacts not only with the nearest inclusion but also with the surrounding ones. The three-phase (fiber/interphase/matrix) model introduced by Christenson and Lo [9]

F. M. Chen (✉)
Department of Mechanical Engineering, Nan Kai University of Technology,
568 Chung Cheng Road, Tsao Tun 542, Nantou, Taiwan
E-mail: fmchen@nkut.edu.tw

is of great practical and theoretical interest in composite mechanics research. Luo and Chen [10] evaluated the interaction energy and the force acting on an edge dislocation when dislocation was located inside the interphase layer based on the Laurent series expansion. Xiao and Chen [11] investigated the interaction between an edge and a coated circular inclusion with the Muskhelishvili complex method. Shen et al. [12] solved the anti-plane problem for a screw dislocation in a three-phase elliptical medium by using the conformal mapping and alternating technique. Chao et al. [13] employed the analytical continuation method and alternating technique to solve the plane elasticity problem for an arbitrary point singularity in a three-phase composite cylinder.

In this study, the interaction of an edge dislocation with a nonuniformly coated circular inclusion is investigated. One of the objectives of this study is to develop an effective analytical methodology to construct the full-field solution for this problem. The proposed method is based on the technique of analytical continuation that is alternatively applied across all interfaces in order to derive the solution of the composite in a series form from the corresponding homogeneous solution. Following the brief introduction, the general formulation for plane elasticity and the method of conformal mapping are described in Sect. 2. The series form solutions for the complex stress potentials are given in Sect. 3. Then, some numerical examples are given to discuss the effect of the nonuniformity of the interphase thickness and combination of material constants on the image force in Sect. 4. Finally, Sect. 5 concludes this article.

2 Problem formulation

Consider a circular inclusion S_a surrounded by an interphase layer S_b of nonuniform thickness, which in turn is embedded in an unbounded matrix S_c (see Fig. 1). The shear moduli of S_a , S_b and S_c are, respectively, G_a , G_b and G_c . Both the outer circular interface L_2 formed by S_c and S_b , and the inner circular interface L_1 formed by S_a and S_b are assumed to be perfect, i.e. both tractions and displacements are continuous across the two interfaces. The origin of the Cartesian coordinate system is chosen to be at the center of the outer circle L_2 of unit radius. The center of the inner circle L_1 of radius $R_0 = (x_2 - x_1)/2$ lies on the x -axis. The two centers of the two circles L_1 and L_2 are set apart by the distance $\Delta = (x_1 + x_2)/2$. An edge dislocation is located at the point $z_0 = x_0 + iy_0$ in the matrix. The components of the displacements, stresses and tractions for an isotropic body under plane deformation are expressed in terms of two complex functions $\phi(z)$ and $\psi(z)$, as follows [14]:

$$2G(u_x + iu_y) = \kappa\phi(z) - z\overline{\phi'(z)} - \overline{\psi(z)} \quad (1)$$

$$\sigma_{xx} + \sigma_{yy} = 2[\phi'(z) + \overline{\phi'(z)}] \quad (2)$$

$$\sigma_{yy} - \sigma_{xx} + 2i\sigma_{xy} = 2[\bar{z}\phi''(z) + \psi'(z)] \quad (3)$$

$$-F_y + iF_x = \phi(z) + z\overline{\phi'(z)} + \overline{\psi(z)} \quad (4)$$

where $\kappa = 3 - 4\nu$ for the plane strain deformation and $(3 - \nu)/(1 + \nu)$ for the plane stress deformation, ν and G are Poisson's ratio and the shear modulus, respectively. Here, the prime represents the derivative with respect to $z = x + iy$, and the overbar represents the complex conjugate.

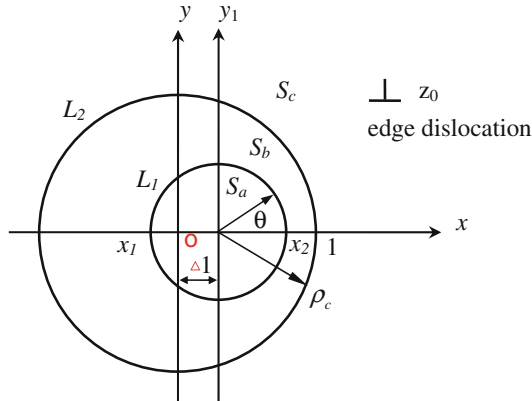


Fig. 1 An edge dislocation and a nonuniformly coated circular inclusion

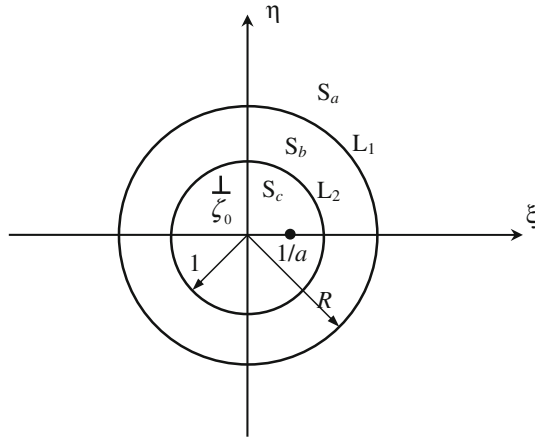


Fig. 2 The problem in the ξ -plane

We adopt the following conformal mapping function $m(\zeta)$ [15]

$$z = m(\zeta) = \frac{\zeta - a}{a\zeta - 1} \quad (5)$$

where

$$a = \frac{1 + x_1 x_2 + \sqrt{(x_1^2 - 1)(x_2^2 - 1)}}{x_1 + x_2} > 1$$

The mapped ζ plane is shown in Fig. 2. It can be observed that the unbounded matrix S_c is mapped onto a unit disk $|\zeta| < 1$, the interphase layer S_b formed by two eccentric circles L_1 and L_2 is mapped onto the annulus $1 < |\zeta| < R$ ($R = (1 - x_1 x_2 + \sqrt{(x_1^2 - 1)(x_2^2 - 1)}) / (x_2 - x_1) > 1$), and the circular inclusion S_a is mapped onto $|\zeta| > R$ in the ζ -plane. For convenience, we write $\phi(\zeta) = \phi(m(\zeta))$ and $\psi(\zeta) = \psi(m(\zeta))$ so that in the mapped ζ -plane, the displacements, stresses and resultant forces take the form

$$2G(u_x + iu_y) = \kappa\phi(\zeta) - \frac{m(\zeta)}{m'(\zeta)}\overline{\phi'(\zeta)} - \overline{\psi(\zeta)} \quad (6)$$

$$\sigma_{xx} + \sigma_{yy} = 2 \left\{ \frac{\phi'(\zeta)}{m'(\zeta)} + \frac{\overline{\phi'(\zeta)}}{m'(\zeta)} \right\} \quad (7)$$

$$\sigma_{yy} - \sigma_{xx} + 2i\sigma_{xy} = 2 \left[\frac{\overline{m(\zeta)}}{m'(\zeta)} \frac{d}{d\zeta} \left\{ \frac{\phi'(\zeta)}{m'(\zeta)} \right\} + \frac{\psi'(\zeta)}{m'(\zeta)} \right] \quad (8)$$

$$-F_y + iF_x = \phi(\zeta) + \frac{m(\zeta)}{m'(\zeta)}\overline{\phi'(\zeta)} + \overline{\psi(\zeta)} \quad (9)$$

3 Stress fields

The complex potentials for an edge dislocation at $z = z_0$ in an infinite homogeneous plane can be trivially given as

$$\phi_0(\zeta) = Q \log \left[\frac{(a^2 - 1)(\zeta - \zeta_0)}{(a\zeta - 1)(a\zeta_0 - 1)} \right] \quad (10)$$

$$\psi_0(\zeta) = \overline{Q} \log \left[\frac{(a^2 - 1)(\zeta - \zeta_0)}{(a\zeta - 1)(a\zeta_0 - 1)} \right] - Q \frac{(a\zeta - 1)(a\zeta_0 - 1)(\overline{\zeta_0} - a)}{(a^2 - 1)(\zeta - \zeta_0)(a\overline{\zeta_0} - 1)} \quad (11)$$

where $Q = \frac{G(b_x + ib_y)}{\pi i(1+\kappa)}$, and b_x and b_y are the Cartesian components of Burgers vector.

For a region bounded by a circle, say $c = |\zeta|$, we introduce an auxiliary stress function $\omega(\zeta)$ such that

$$\omega(\zeta) = \frac{\bar{m}\left(\frac{c^2}{\zeta}\right)}{m'(\zeta)}\phi'(\zeta) + \psi(\zeta) \quad (12)$$

It should be noticed that unlike the standard Muskhelishvili complex functions $\phi(\zeta)$ and $\psi(\zeta)$, the function $\omega(\zeta)$ is dependent on the radius of any circular interface.

The stress functions for a nonuniformly coated circular inclusion embedded in an infinite matrix subject to an edge dislocation can be assumed as

$$\phi(\zeta) = \begin{cases} \sum_{n=1}^{\infty} \phi_{an}(\zeta) & \zeta \in S_a \\ \sum_{n=1}^{\infty} \phi_n(\zeta) + \sum_{n=1}^{\infty} \phi_{bn}(\zeta) & \zeta \in S_b \\ \phi_0(\zeta) + \sum_{n=1}^{\infty} \phi_{cn}(\zeta) & \zeta \in S_c \end{cases} \quad (13)$$

$$\omega(\zeta) = \begin{cases} \sum_{n=1}^{\infty} \omega_{an}(\zeta) & \zeta \in S_a \\ \sum_{n=1}^{\infty} \omega_n(\zeta) + \sum_{n=1}^{\infty} \omega_{bn}(\zeta) & \zeta \in S_b \\ \omega_0(\zeta) + \sum_{n=1}^{\infty} \omega_{cn}(\zeta) & \zeta \in S_c \end{cases} \quad (14)$$

The alternating technique and the analytical continuation method are applied to derive the unknown stress functions as follows.

Step 1: Analytical continuation across L_2

We first introduce two pairs of stress functions $\phi_{c1}(\zeta), \omega_{c1}(\zeta)$ and $\phi_1(\zeta), \omega_1(\zeta)$, respectively, holomorphic except some singular points in $|\zeta| \leq 1$ and $|\zeta| \geq 1$ to satisfy the continuity conditions along L_2 .

$$\phi_{c1}(\sigma) + \overline{\omega_{c1}(\sigma)} + \phi_0(\sigma) + \overline{\omega_0(\sigma)} = \phi_1(\sigma) + \overline{\omega_1(\sigma)} \quad \sigma \in L_2 \quad (15)$$

$$\frac{1}{G_c} \left[\kappa_c \phi_{c1}(\sigma) - \overline{\omega_{c1}(\sigma)} + \kappa_c \phi_0(\sigma) - \overline{\omega_0(\sigma)} \right] = \frac{1}{G_b} \left[\kappa_b \phi_1(\sigma) - \overline{\omega_1(\sigma)} \right] \quad \sigma \in L_2 \quad (16)$$

where $\omega_0(\zeta) = \frac{\bar{m}\left(\frac{1}{\zeta}\right)}{m'(\zeta)}\phi'_0(\zeta) + \psi_0(\zeta)$, and the elastic constants involved in $\phi_0(\zeta)$ and $\psi_0(\zeta)$ are for region S_c .

By the standard analytical continuation arguments it follows that

$$\phi_{c1}(\zeta) - \overline{\omega_1}\left(\frac{1}{\zeta}\right) + \overline{\omega_0}\left(\frac{1}{\zeta}\right) + \frac{(a^2 - 1)^2}{a^3(a\zeta - 1)}C_0 - \frac{(a^2 - 1)^2}{a^3(a\zeta - 1)}C_1 = 0 \quad |\zeta| \leq 1 \quad (17)$$

$$\phi_1(\zeta) - \phi_0(\zeta) - \overline{\omega_{c1}}\left(\frac{1}{\zeta}\right) + \frac{(a^2 - 1)^2}{a^3(a\zeta - 1)}C_0 - \frac{(a^2 - 1)^2}{a^3(a\zeta - 1)}C_1 = 0 \quad |\zeta| \geq 1 \quad (18)$$

$$\frac{\kappa_c}{G_c} \phi_{c1}(\zeta) + \frac{1}{G_b} \overline{\omega_1}\left(\frac{1}{\zeta}\right) - \frac{1}{G_c} \overline{\omega_0}\left(\frac{1}{\zeta}\right) - \frac{(a^2 - 1)^2}{a^3(a\zeta - 1)} \left(\frac{C_0}{G_c} - \frac{C_1}{G_b} \right) = 0 \quad |\zeta| \leq 1 \quad (19)$$

$$\frac{\kappa_b}{G_b} \phi_1(\zeta) - \frac{\kappa_c}{G_c} \phi_0(\zeta) + \frac{1}{G_c} \overline{\omega_{c1}}\left(\frac{1}{\zeta}\right) - \frac{(a^2 - 1)^2}{a^3(a\zeta - 1)} \left(\frac{C_0}{G_c} - \frac{C_1}{G_b} \right) = 0 \quad |\zeta| \geq 1 \quad (20)$$

where $C_0 = a^2 \overline{\phi'_0}(a)$, $C_1 = a^2 \overline{\phi'_1}(a)$.

Solve Eqs. (17)–(20) to yield

$$\phi_{c1}(\zeta) = \Pi_{bc} \overline{\omega_0}\left(\frac{1}{\zeta}\right) + \Pi_{bc} \frac{(a^2 - 1)^2 C_0}{a^3(a\zeta - 1)} \quad (21)$$

$$\omega_1(\zeta) = (1 + \Pi_{bc})\omega_0(\zeta) + (1 + \Pi_{bc}) \frac{(a^2 - 1)^2}{a^3\left(\frac{a}{\zeta} - 1\right)} \overline{C_0} - \frac{(a^2 - 1)^2}{a^3\left(\frac{a}{\zeta} - 1\right)} \overline{C_1} \quad (22)$$

$$\phi_1(\zeta) = (1 + \Lambda_{bc})\phi_0(\zeta) - \Pi_{cb} \frac{(a^2 - 1)^2}{a^3(a\zeta - 1)} C_1 \quad (23)$$

$$\omega_{c1}(\zeta) = \Lambda_{bc} \overline{\phi_0} \left(\frac{1}{\zeta} \right) + \frac{(a^2 - 1)^2}{a^3 \left(\frac{a}{\zeta} - 1 \right)} \overline{C_0} - (1 + \Pi_{cb}) \frac{(a^2 - 1)^2}{a^3 \left(\frac{a}{\zeta} - 1 \right)} \overline{C_1} \quad (24)$$

where $\Lambda_{bc} = \frac{G_b \kappa_c - G_c \kappa_b}{G_b + G_c \kappa_b}$, $\Pi_{bc} = \frac{G_b - G_c}{G_b \kappa_c + G_c}$
Step 2: Analytical continuation across L_1

Since the fields produced by $\phi_{c1}(\zeta)$ and $\omega_{c1}(\zeta)$ cannot satisfy the continuity condition at L_1 , two pairs of stress functions $\phi_{b1}(\zeta), \omega_{b1}(\zeta)$ and $\phi_{a1}(\zeta), \omega_{a1}(\zeta)$, respectively, holomorphic except some singular points in $|\zeta| \leq R$ and $|\zeta| \geq R$ are introduced to satisfy the continuity condition along L_1 that

$$\phi_1(\sigma) + \overline{\omega_1^*(\sigma)} + \phi_{b1}(\sigma) + \overline{\omega_{b1}(\sigma)} = \phi_{a1}(\sigma) + \overline{\omega_{a1}(\sigma)} \quad \sigma \in L_1 \quad (25)$$

$$\frac{1}{G_b} \left[\kappa_b \phi_1(\sigma) - \overline{\omega_1^*(\sigma)} + \kappa_b \phi_{b1}(\sigma) - \overline{\omega_{b1}(\sigma)} \right] = \frac{1}{G_a} \left[\kappa_a \phi_{a1}(\sigma) - \overline{\omega_{a1}(\sigma)} \right] \quad \sigma \in L_1 \quad (26)$$

where $\omega_1^*(\zeta) = \omega_1(\zeta) + \frac{\overline{m}\left(\frac{R^2}{\zeta}\right) - \overline{m}\left(\frac{1}{\zeta}\right)}{m'(\zeta)} \phi_1'(\zeta)$.

By the standard analytical continuation arguments it follows that

$$\phi_{b1}(\zeta) + \overline{\omega_1^*} \left(\frac{R^2}{\zeta} \right) - \overline{\omega_{a1}} \left(\frac{R^2}{\zeta} \right) + \frac{(a^2 R^2 - 1)^2 C_1^*}{a^3(a\zeta - 1)} - \frac{(a^2 R^2 - 1)^2 C_{a1}}{a^3(a\zeta - 1)} = 0 \quad |\zeta| \leq R \quad (27)$$

$$\phi_{a1}(\zeta) - \phi_1(\zeta) - \overline{\omega_{b1}} \left(\frac{R^2}{\zeta} \right) + \frac{(a^2 R^2 - 1)^2 C_1^*}{a^3(a\zeta - 1)} - \frac{(a^2 R^2 - 1)^2 C_{a1}}{a^3(a\zeta - 1)} = 0 \quad |\zeta| \geq R \quad (28)$$

$$\frac{\kappa_b}{G_b} \phi_{b1}(\zeta) - \frac{1}{G_b} \overline{\omega_1^*} \left(\frac{R^2}{\zeta} \right) + \frac{1}{G_a} \overline{\omega_{a1}} \left(\frac{R^2}{\zeta} \right) - \frac{1}{G_b} \frac{(a^2 R^2 - 1)^2 C_1^*}{a^3(a\zeta - 1)} + \frac{1}{G_a} \frac{(a^2 R^2 - 1)^2 C_{a1}}{a^3(a\zeta - 1)} \quad |\zeta| \leq R \quad (29)$$

$$\frac{\kappa_a}{G_a} \phi_{a1}(\zeta) + \frac{1}{G_b} \overline{\omega_{b1}} \left(\frac{R^2}{\zeta} \right) - \frac{\kappa_b}{G_b} \phi_1(\zeta) - \frac{1}{G_b} \frac{(a^2 R^2 - 1)^2 C_1^*}{a^3(a\zeta - 1)} + \frac{1}{G_a} \frac{(a^2 R^2 - 1)^2 C_{a1}}{a^3(a\zeta - 1)} = 0 \quad |\zeta| \geq R \quad (30)$$

Solve Eqs. (27)–(30) to yield

$$\phi_{b1}(\zeta) = \Pi_{ab} \overline{\omega_1^*} \left(\frac{R^2}{\zeta} \right) + \Pi_{ab} \frac{(a^2 R^2 - 1)^2 C_1^*}{a^3(a\zeta - 1)} \quad (31)$$

$$\omega_{a1}(\zeta) = (1 + \Pi_{ab}) \omega_1^*(\zeta) + (1 + \Pi_{ab}) \frac{(a^2 R^2 - 1)^2 \overline{C_1^*}}{a^3 \left(a \frac{R^2}{\zeta} - 1 \right)} - \frac{(a^2 R^2 - 1)^2 \overline{C_{a1}}}{a^3 \left(a \frac{R^2}{\zeta} - 1 \right)} \quad (32)$$

$$\phi_{a1}(\zeta) = (1 + \Lambda_{ab}) \phi_1(\zeta) - \Pi_{ba} \frac{(a^2 R^2 - 1)^2 C_{a1}}{a^3(a\zeta - 1)} \quad (33)$$

$$\omega_{b1}(\zeta) = \Lambda_{ab} \overline{\phi_1} \left(\frac{R^2}{\zeta} \right) + \frac{(a^2 R^2 - 1)^2 \overline{C_1^*}}{a^3 \left(a \frac{R^2}{\zeta} - 1 \right)} - (1 + \Pi_{ba}) \frac{(a^2 R^2 - 1)^2 \overline{C_{a1}}}{a^3 \left(a \frac{R^2}{\zeta} - 1 \right)} \quad (34)$$

where $C_{a1} = a^2 \overline{\phi_{a1}'}(R^2 a)$, $C_1^* = a^2 \overline{\phi_1'}(R^2 a)$.

Step 3: Analytical continuation across L_2

Since the stress functions $\phi_{b1}(\zeta)$ and $\omega_{b1}(\zeta)$ cannot satisfy the continuity condition at L_2 , two pairs of stress functions $\phi_{c2}(\zeta), \omega_{c2}(\zeta)$ and $\phi_2(\zeta), \omega_2(\zeta)$, respectively, holomorphic except some singular points in $|\zeta| \leq 1$ and $|\zeta| \geq 1$ are introduced to satisfy the continuity condition along L_2 that

$$\phi_{c2}(\sigma) + \overline{\omega_{c2}(\sigma)} = \phi_{b1}(\sigma) + \overline{\omega_{b1}^*(\sigma)} + \phi_2(\sigma) + \overline{\omega_2(\sigma)} \quad \sigma \in L_2 \quad (35)$$

$$\frac{\kappa_c}{G_c} \phi_{c2}(\sigma) - \frac{1}{G_c} \overline{\omega_{c2}(\sigma)} = \frac{\kappa_b}{G_b} \phi_{b1}(\sigma) - \frac{1}{G_b} \overline{\omega_{b1}^*(\sigma)} + \frac{\kappa_b}{G_b} \phi_2(\sigma) - \frac{1}{G_b} \overline{\omega_2(\sigma)} \quad \sigma \in L_2 \quad (36)$$

where

$$\omega_{b1}^*(\zeta) = \omega_{b1}(\zeta) + \frac{\overline{m}\left(\frac{1}{\zeta}\right) - \overline{m}\left(\frac{R^2}{\zeta}\right)}{m'(\zeta)} \phi'_{b1}(\zeta).$$

By the analytical continuation method, we have

$$\phi_{c2}(\zeta) - \phi_{b1}(\zeta) - \overline{\omega_2}\left(\frac{1}{\zeta}\right) - \frac{(a^2 - 1)^2}{a^3(a\zeta - 1)} C_2 = 0 \quad |\zeta| \leq 1 \quad (37)$$

$$\phi_2(\zeta) - \overline{\omega_{c2}}\left(\frac{1}{\zeta}\right) + \overline{\omega_{b1}^*}\left(\frac{1}{\zeta}\right) - \frac{(a^2 - 1)^2}{a^3(a\zeta - 1)} C_2 = 0 \quad |\zeta| \geq 1 \quad (38)$$

$$\frac{\kappa_c}{G_c} \phi_{c2}(\zeta) - \frac{\kappa_b}{G_b} \phi_{b1}(\zeta) + \frac{1}{G_b} \overline{\omega_2}\left(\frac{1}{\zeta}\right) + \frac{1}{G_b} \frac{(a^2 - 1)^2}{a^3(a\zeta - 1)} C_2 = 0 \quad |\zeta| \leq 1 \quad (39)$$

$$\frac{\kappa_b}{G_b} \phi_2(\zeta) + \frac{1}{G_c} \overline{\omega_{c2}}\left(\frac{1}{\zeta}\right) - \frac{1}{G_b} \overline{\omega_{b1}^*}\left(\frac{1}{\zeta}\right) + \frac{1}{G_b} \frac{(a^2 - 1)^2}{a^3(a\zeta - 1)} C_2 = 0 \quad |\zeta| \geq 1 \quad (40)$$

Solve Eqs. (37)–(40) to yield

$$\phi_{c2}(\zeta) = (1 + \Lambda_{cb}) \phi_{b1}(\zeta) \quad (41)$$

$$\omega_2(\zeta) = \Lambda_{cb} \overline{\phi_{b1}}\left(\frac{1}{\zeta}\right) - \frac{(a^2 - 1)^2 \overline{C_2}}{a^3 \left(\frac{a}{\zeta} - 1\right)} \quad (42)$$

$$\phi_2(\zeta) = \Pi_{cb} \overline{\omega_{b1}^*}\left(\frac{1}{\zeta}\right) - \Pi_{cb} \frac{(a^2 - 1)^2 C_2}{a^3(a\zeta - 1)} \quad (43)$$

$$\omega_{c2}(\zeta) = (1 + \Pi_{cb}) \omega_{b1}^*(\zeta) - (1 + \Pi_{cb}) \frac{(a^2 - 1)^2 \overline{C_2}}{a^3 \left(\frac{a}{\zeta} - 1\right)} \quad (44)$$

where $C_2 = a^2 \overline{\phi'_2}(a)$

By repetitions of the previous two steps to satisfy the continuity conditions at L_1 and L_2 , one can find all the unknown functions that can be expressed in terms of $\phi_0(\zeta)$ and $\omega_0(\zeta)$.

$$\phi(\zeta) = \begin{cases} (1 + \Lambda_{ab}) \sum_{n=1}^{\infty} \phi_n(\zeta) - \frac{(1 + \Lambda_{ab}) \Pi_{ba}}{1 - \Pi_{ba}^2} \left[\sum_{n=1}^{\infty} C_n^* + \Pi_{ba} \sum_{n=1}^{\infty} \overline{C_n^*} \right] h(\zeta) & \zeta \in S_a \\ \sum_{n=1}^{\infty} \phi_n(\zeta) + \Lambda_{cb}^{-1} \left[\sum_{n=1}^{\infty} \overline{\omega_{n+1}}\left(\frac{1}{\zeta}\right) + u(\zeta) \sum_{n=1}^{\infty} C_{n+1} \right] & \zeta \in S_b \\ \phi_0(\zeta) + \Pi_{bc} \left[\overline{\omega_0}\left(\frac{1}{\zeta}\right) + u(\zeta) C_0 \right] + (1 + \Lambda_{cb}^{-1}) \left[\sum_{n=1}^{\infty} \overline{\omega_{n+1}}\left(\frac{1}{\zeta}\right) + u(\zeta) \sum_{n=1}^{\infty} C_{n+1} \right] & \zeta \in S_c \end{cases} \quad (45)$$

$$\omega(\zeta) = \begin{cases} (1 + \Pi_{ab}) \sum_{n=1}^{\infty} [\omega_n(\zeta) + t_{21}(\zeta) \phi'_n(\zeta)] \\ - \frac{\Lambda_{ab} - \Pi_{ab} + \Pi_{ba}^2(1 + \Pi_{ab})}{1 - \Pi_{ba}^2} \bar{h}\left(\frac{R^2}{\zeta}\right) \sum_{n=1}^{\infty} \bar{C}_n^* - \frac{\Pi_{ba}(1 + \Lambda_{ab})}{1 - \Pi_{ba}^2} \bar{h}\left(\frac{R^2}{\zeta}\right) \sum_{n=1}^{\infty} C_n^* & \zeta \in S_a \\ \sum_{n=1}^{\infty} \omega_n(\zeta) + \Pi_{cb}^{-1} \sum_{n=1}^{\infty} \bar{\phi}_{n+1}\left(\frac{1}{\zeta}\right) + t_{12}(\zeta) \Lambda_{cb}^{-1} \left[\frac{1}{\zeta^2} \sum_{n=1}^{\infty} \bar{\omega}'_{n+1}\left(\frac{1}{\zeta}\right) - u'(\zeta) \sum_{n=1}^{\infty} C_{n+1} \right] \\ + \bar{u}\left(\frac{1}{\zeta}\right) \sum_{n=1}^{\infty} \bar{C}_{n+1} & \zeta \in S_b \\ \omega_0(\zeta) + \Lambda_{bc} \bar{\phi}_0\left(\frac{1}{\zeta}\right) + \bar{u}\left(\frac{1}{\zeta}\right) \bar{C}_0 - (1 + \Pi_{cb}) \bar{u}\left(\frac{1}{\zeta}\right) \bar{C}_1 + (1 + \Pi_{cb}^{-1}) \sum_{n=1}^{\infty} \bar{\phi}_{n+1}\left(\frac{1}{\zeta}\right) & \zeta \in S_c \end{cases} \quad (46)$$

$$\text{where } t_{12}(\zeta) = -t_{21}(\zeta) = \frac{\bar{m}\left(\frac{1}{\zeta}\right) - \bar{m}\left(\frac{R^2}{\zeta}\right)}{m'(\zeta)}$$

$$u(\zeta) = \frac{(a^2 - 1)^2}{a^3(a\zeta - 1)}, \quad h(\zeta) = \frac{(a^2 R^2 - 1)^2}{a^3(a\zeta - 1)}$$

$$C_n = a^2 \bar{\phi}'_n(a), \quad C_n^* = a^2 \bar{\phi}'_n(R^2 a)$$

and the recurrence formulae for $\phi_n(\zeta)$ and $\omega_n(\zeta)$ are

$$\phi_{n+1}(\zeta) = \begin{cases} (1 + \Lambda_{bc})\phi_0(\zeta) - \Pi_{cb}u(\zeta)C_1 & \text{for } n = 0 \\ + \Pi_{cb}\Lambda_{ab}\phi_n(R^2\zeta) - \frac{\Pi_{cb}\Pi_{ba}(1 + \Lambda_{ab})\bar{C}_n^*h(R^2\zeta)}{1 - \Pi_{ba}} - \frac{\Pi_{cb}(\Lambda_{ab} + \Pi_{ba})C_n^*h(R^2\zeta)}{1 - \Pi_{ba}} \\ - \Pi_{cb}\Pi_{ab}R^2\zeta^2\bar{t}_{12}\left(\frac{1}{\zeta}\right) [\omega'_n(R^2\zeta) + t'_{21}(R^2\zeta)\phi'_n(R^2\zeta) + t_{21}(R^2\zeta)\phi''_n(R^2\zeta)] \\ + \Pi_{cb}\Pi_{ab}\bar{t}_{12}\left(\frac{1}{\zeta}\right)\bar{h}'\left(\frac{1}{\zeta}\right)\bar{C}_n^* - \Pi_{cb}u(\zeta)C_{n+1} & \text{for } n = 1, 2, 3 \dots \end{cases} \quad (47)$$

$$\omega_{n+1}(\zeta) = \begin{cases} (1 + \Pi_{bc})\omega_0(\zeta) + \bar{u}\left(\frac{1}{\zeta}\right) [(1 + \Pi_{bc})\bar{C}_0 - \bar{C}_1] & \text{for } n = 0 \\ \Lambda_{cb}\Pi_{ab} [\omega_n(R^2\zeta) + t_{21}(R^2\zeta)\phi'_n(R^2\zeta) + \bar{h}\left(\frac{1}{\zeta}\right)\bar{C}_n^*] - \bar{u}\left(\frac{1}{\zeta}\right)\bar{C}_{n+1} & \text{for } n = 1, 2, 3 \dots \end{cases} \quad (48)$$

Using Eqs. (45) and (46) and the relations

$$\psi_n(\zeta) = \omega_n(\zeta) - \frac{\bar{m}\left(\frac{1}{\zeta}\right)}{m'(\zeta)}\phi'_n(\zeta)$$

$$\psi_{an}(\zeta) = \omega_{an}(\zeta) - \frac{\bar{m}\left(\frac{R^2}{\zeta}\right)}{m'(\zeta)}\phi'_{an}(\zeta)$$

$$\psi_{bn}(\zeta) = \omega_{bn}(\zeta) - \frac{\bar{m}\left(\frac{R^2}{\zeta}\right)}{m'(\zeta)}\phi'_{bn}(\zeta)$$

$$\psi_{cn}(\zeta) = \omega_{cn}(\zeta) - \frac{\bar{m}\left(\frac{1}{\zeta}\right)}{m'(\zeta)}\phi'_{cn}(\zeta)$$

we can find the complete series solution of $\phi(\zeta)$ and $\psi(\zeta)$.

For a limiting case when the thickness of the interphase layer is uniform, i.e., $a \rightarrow \infty$ and $R_0 = 1/R$, then

$$\begin{aligned} z &= m(\zeta) = -\frac{1}{\zeta} \\ \phi'(\zeta) &= z^2 \phi'(z) \\ u(\zeta) &= \frac{1}{\zeta}, \quad h(\zeta) = \frac{1}{R_0^4 \zeta} \\ C_n^* &= R_0^4 C_n \end{aligned}$$

Equations (45) and (46) can be simplified to

$$\begin{aligned} \phi(\zeta) &= \begin{cases} (1 + \Lambda_{ab}) \sum_{n=1}^{\infty} \phi_n(z) + \frac{(1+\Lambda_{ab})\Pi_{ba}}{1-\Pi_{ba}^2} [\sum_{n=1}^{\infty} C_n + \Pi_{ba} \sum_{n=1}^{\infty} \bar{C}_n] z & z \in S_a \\ \sum_{n=1}^{\infty} \phi_n(z) + \Lambda_{cb}^{-1} \left[\sum_{n=1}^{\infty} \bar{\omega}_{n+1} \left(\frac{1}{z} \right) - z \sum_{n=1}^{\infty} C_{n+1} \right] & z \in S_b \\ \phi_0(z) + \Pi_{bc} \left[\bar{\omega}_0 \left(\frac{1}{z} \right) - C_0 z \right] + (1 + \Lambda_{cb}^{-1}) \left[\sum_{n=1}^{\infty} \bar{\omega}_{n+1} \left(\frac{1}{z} \right) - z \sum_{n=1}^{\infty} C_{n+1} \right] & z \in S_c \end{cases} \quad (49) \\ \omega(\zeta) &= \begin{cases} (1 + \Pi_{ab}) \sum_{n=1}^{\infty} \left[\omega_n(z) + \frac{(R_0^2-1)}{z} \phi'_n(z) \right] \\ + \frac{\Lambda_{ab}-\Pi_{ab}+\Pi_{ba}^2(1+\Pi_{ab})}{1-\Pi_{ba}^2} \frac{R_0^2}{z} \sum_{n=1}^{\infty} \bar{C}_n + \frac{\Pi_{ba}(1+\Lambda_{ab})}{1-\Pi_{ba}^2} \frac{R_0^2}{z} \sum_{n=1}^{\infty} C_n & z \in S_a \\ \sum_{n=1}^{\infty} \omega_n(z) + \Pi_{cb}^{-1} \sum_{n=1}^{\infty} \bar{\phi}_{n+1} \left(\frac{1}{z} \right) + \frac{(1-R_0^2)\Lambda_{cb}^{-1}}{z} \left[\frac{1}{z^2} \sum_{n=1}^{\infty} \bar{\omega}'_{n+1} \left(\frac{1}{z} \right) + \sum_{n=1}^{\infty} C_{n+1} \right] \\ - \frac{1}{z} \sum_{n=1}^{\infty} \bar{C}_{n+1} & z \in S_b \\ \omega_0(z) + \Lambda_{bc} \bar{\phi}_0 \left(\frac{1}{z} \right) - \frac{1}{z} \bar{C}_0 + (1 + \Pi_{cb}) \frac{1}{z} \bar{C}_1 + (1 + \Pi_{cb}^{-1}) \sum_{n=1}^{\infty} \bar{\phi}_{n+1} \left(\frac{1}{z} \right) & z \in S_c \end{cases} \quad (50) \end{aligned}$$

where $C_n = \bar{\phi}'_n(0)$, and the recurrence formulae for $\phi_n(z)$ and $\omega_n(z)$ are

$$\phi_{n+1}(z) = \begin{cases} (1 + \Lambda_{bc})\phi_0(z) + \Pi_{cb}zC_1 & \text{for } n = 0 \\ \Pi_{cb}\Lambda_{ab}\phi_n(R_0^2z) + \frac{(1+\Lambda_{ab})\Pi_{cb}\Pi_{ba}\bar{C}_nR_0^2z}{1-\Pi_{ba}} + \frac{(\Lambda_{ab}+\Pi_{ba})\Pi_{cb}C_nR_0^2z}{1-\Pi_{ba}} \\ + \Pi_{cb}\Pi_{ab}R_0^2(R_0^2-1)z^3 \left[\omega'_n(R_0^2z) - \frac{(R_0^2-1)}{R_0^4z^2}\phi'_n(R_0^2z) + \frac{(R_0^2-1)}{R_0^2z}\phi''(R_0^2z) \right] \\ + \Pi_{cb}\Pi_{ab}(R_0^2-1)z\bar{C}_n + \Pi_{cb}zC_{n+1} & \text{for } n = 1, 2, 3 \dots \end{cases} \quad (51)$$

$$\omega_{n+1}(z) = \begin{cases} (1 + \Pi_{bc})\omega_0(z) - \frac{1}{z} [(1 + \Pi_{bc})\bar{C}_0 - \bar{C}_1] & \text{for } n = 0 \\ \Lambda_{cb}\Pi_{ab} \left[\omega_n(R_0^2z) + \frac{(R_0^2-1)}{zR_0^2}\phi'_n(R_0^2z) - \frac{\bar{C}_n}{z} \right] + \frac{\bar{C}_{n+1}}{z} & \text{for } n = 1, 2, 3 \dots \end{cases} \quad (52)$$

which are in agreement with the results provided by Chao et al. [13].

4 Numerical results and discussions

In this section, we will investigate the effect of the material combinations and varying interphase thickness on the dislocation force. The image force acting on the dislocation can be calculated through the Peach–Koehler formula [16].

$$F_x + iF_y = (\sigma_{xy}^* b_x + \sigma_{yy}^* b_y) - i(\sigma_{xx}^* b_x + \sigma_{xy}^* b_y) \quad (53)$$

where σ_{xx}^* , σ_{yy}^* and σ_{xy}^* are the components of the perturbation stress at the dislocation in the Cartesian coordinates.

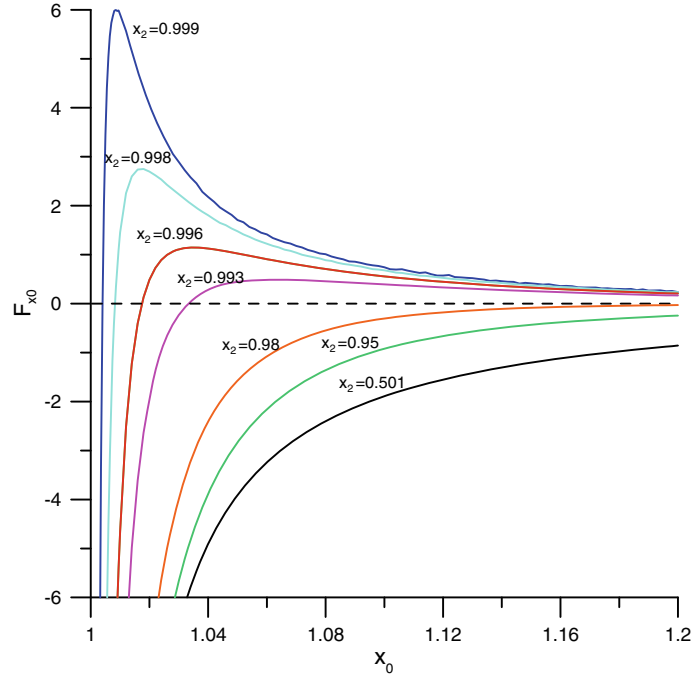


Fig. 3 Normalized force on sliding dislocation F_{x0} vs. the dislocation location and x_2 for $R_0 = 0.5$, $G_a : G_b : G_c = 4 : 2 : 3$ and $\nu_a = \nu_b = \nu_c = 0.3$

We now define the normalized forces on the dislocation as

$$F_{x0} = \pi(1 + \kappa_c)\rho_c F_1 / G_c b_x^2 \quad (54)$$

$$F_{y0} = \pi(1 + \kappa_c)\rho_c F_2 / G_c b_y^2 \quad (55)$$

where F_1 is the force on the gliding dislocation b_x (Burgers vector $(b_x, 0)$), and F_2 is the force on the climbing dislocation b_y (Burgers vector $(0, b_y)$).

The stress functions for a nonuniformly coated circular inclusion in an unbounded matrix subjected to an edge dislocation as indicated in Eqs. (45) and (46) are expressed in terms of $\phi_n(\zeta)$ and $\omega_n(\zeta)$ ($n = 1, 2, 3, \dots$), which may be calculated from a homogeneous solution $\phi_0(\zeta)$ and $\omega_0(\zeta)$ by the recurrence formulae (47) and (48). The rate of convergence depends on the ratios $|\phi_{n+1}(\zeta)| / |\phi_n(\zeta)|$ and $|\omega_{n+1}(\zeta)| / |\omega_n(\zeta)|$, which in turn depend on the nondimensional bimaterial constants Λ_{ab} and Π_{ab} (or Λ_{cb} and Π_{cb}). For most combinations of materials, Λ and Π are less than 1 and 0.5, respectively, which guarantees rapid convergence. Furthermore, the convergence rate becomes more rapid as the differences of the elastic constants of the neighboring materials get smaller. Note that all the following calculated results sum up the first four terms in a series solution, since they are checked to achieve a good accuracy for the current problem.

In the following discussion, we assume the dislocation is located at point $z_0 = (x_0, 0)$. Figures 3 and 4, respectively, show the variation of F_{x0} and F_{y0} versus the dislocation location and x_2 with $G_a : G_b : G_c = 4 : 2 : 3$. This configuration represents that the inclusion is stiffer and the interphase layer is softer than the matrix. One can find an interesting phenomenon when the circle L_1 is very close to L_2 , there exists an unstable equilibrium position that the coated inclusion will first attract the dislocation and then repel it with the increase in the distance between the dislocation and the inclusion. Otherwise, the inclusion has no significant influence on the image force such that the softer interphase layer will always attract the dislocation (negative image force). It is worthy to note that the numerical evaluation shows the contributions of the normalized force for the leading terms of the series solution are approximately 73% ($n = 1$), 19.6% ($n = 2$), 6.7% ($n = 3$) and 0.7% ($n = 4$), respectively. It is likely that the error of approximations with terms up to $n = 4$ is less than 1%. Figures 5 and 6, respectively, show the variation of F_{x0} and F_{y0} versus the dislocation location and x_2 with $G_a : G_b : G_c = 2 : 5 : 3$. This configuration represents that the inclusion is softer and the interphase layer is stiffer than the matrix. We can also find an interesting phenomenon that when the circle L_1 is very

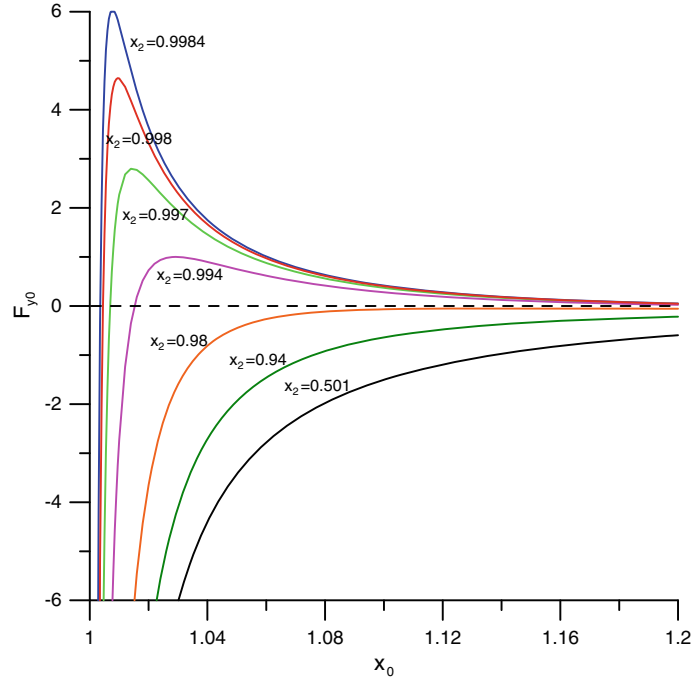


Fig. 4 Normalized force on climbing dislocation F_{y0} vs. the dislocation location and x_2 for $R_0 = 0.5$, $G_a : G_b : G_c = 4 : 2 : 3$ and $v_a = v_b = v_c = 0.3$

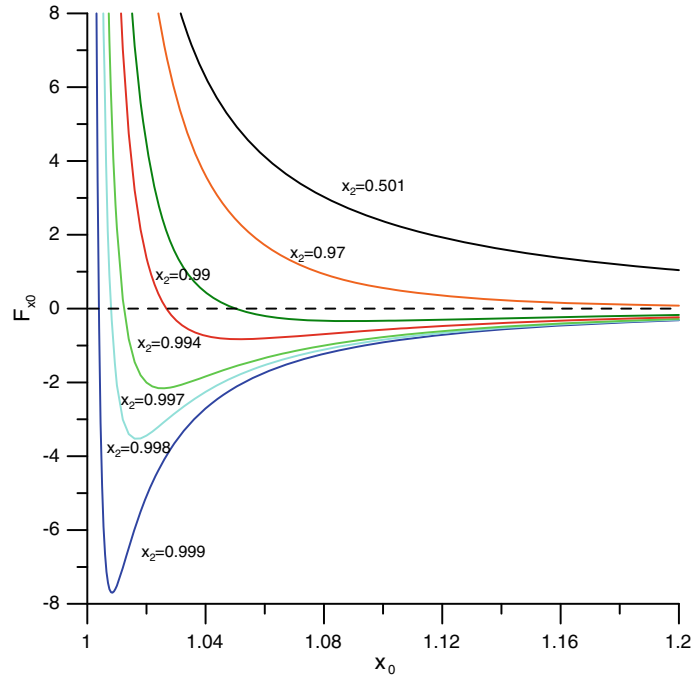


Fig. 5 Normalized force on sliding dislocation F_{x0} vs. the dislocation location and x_2 for $R_0 = 0.5$, $G_a : G_b : G_c = 2 : 5 : 3$ and $v_a = v_b = v_c = 0.3$

close to L_2 , there exists a stable equilibrium position that the coated inclusion will first repel the dislocation and then attract it with the increase in the distance between the dislocation and the inclusion. Otherwise, the inclusion has no significant influence on the image force such that the stiffer interphase layer will always repel the dislocation (positive image force).

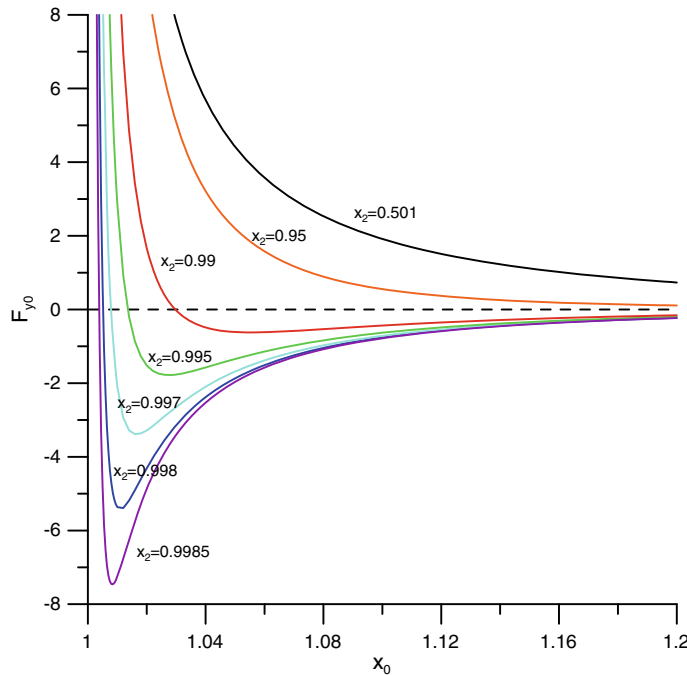


Fig. 6 Normalized force on climbing dislocation F_{y0} vs. the dislocation location and x_2 for $R_0 = 0.5$, $G_a : G_b : G_c = 2 : 5 : 3$ and $v_a = v_b = v_c = 0.3$

5 Conclusion

A novel efficient procedure is established to investigate the interaction between an edge dislocation and a nonuniformly coated circular inclusion. Within the framework of the procedure of analytical continuation and the method of successive approximations, the solution associated with the heterogeneous problem is sought as transformation of the solution to the corresponding homogeneous problem. For a limiting case when the thickness of the interphase layer is uniform, the derived analytical solutions of this paper are reduced to exactly the same results available in the literature. The numerical calculation shows that the nonuniformity of the interphase thickness and combination of material constants have a significant influence on the image force.

Acknowledgments This work was supported by the National Science Council of ROC under the contract number: NSC 97-2221-E-252-006.

References

1. Dondurs, J.: Mathematical theory of dislocations. In: Mura, T. (ed.), ASME: pp. 70–115 (1969)
2. Head, A.K.: The interaction of dislocations and boundaries. *Philos. Mag.* **44**, 92–94 (1953)
3. Fleischer, R.L.: Effects of non-uniformities on the hardening of crystals. *Acta Met.* **8**, 598–604 (1960)
4. Dundurs, J., Mura, T.: Interaction between an edge dislocation and a circular inclusion. *J. Mech. Phys. Solids* **12**, 177–189 (1964)
5. Dundurs, J., Sendeckyj, G.P.: Edge dislocation inside a circular inclusion. *J. Mech. Phys. Solids* **13**, 141–147 (1965)
6. Warren, W.E.: The edge dislocation inside an elliptical inclusion. *Mech. Mater.* **2**, 319–330 (1983)
7. Stagni, L., Lizzio, R.: Shape effects in the interaction between an edge dislocation and elliptical inhomogeneity. *J. Appl. Phys. A* **30**, 217–221 (1983)
8. Santare, M.H., Keer, L.M.: Interaction between an edge dislocation and a rigid elliptical inclusion. *Trans. ASME J. Appl. Mech.* **53**, 382–385 (1986)
9. Christensen, R.M., Lo, K.H.: Solution for effective shear properties in three phase sphere and cylinder models. *J. Mech. Phys. Solids* **27**, 315–330 (1979)
10. Luo, H.A., Chen, Y.: An edge dislocation in a three-phase composite cylinder. *Trans. ASME J. Appl. Mech.* **58**, 75–86 (1991)
11. Xiao, Z.M., Chen, B.J.: On the interaction between an edge dislocation and a coated inclusion. *Int. J. Solids Struct.* **38**, 2533–2548 (2001)
12. Shen, M.H., Chen, S.N., Chen, F.M.: Antiplane study on confocally elliptical inhomogeneity problem using an alternating technique. *Arch. Appl. Mech.* **75**, 302–314 (2006)

-
13. Chao, C.K., Chen, F.M., Shen, M.H.: Circularly cylindrical layered media in plane elasticity. *Int. J. Solids Struct.* **43**, 4739–4756 (2006)
 14. Muskhelishvili, N.I.: Some basic problems of the mathematical theory of elasticity. Noordhoff, Groningen (1953)
 15. Schinzinger, R., Laura, P.A.A.: Conformal mapping: methods and applications. Elsevier, New York (1991)
 16. Hirth, J.P., Lothe, J.: Theory of dislocation. 2nd edn. Wiley, New York (1982)